

See discussions, stats, and author profiles for this publication at: <https://www.researchgate.net/publication/232224367>

Discovery of Inhibitors To Block Interactions of HIV-1 Integrase with Human LEDGF/p75 via Structure-Based Virtual Screening and Bioassays

ARTICLE in JOURNAL OF MEDICINAL CHEMISTRY · OCTOBER 2012

Impact Factor: 5.45 · DOI: 10.1021/jm301226a · Source: PubMed

CITATIONS

17

READS

21

13 AUTHORS, INCLUDING:



[Yaozong Li](#)

Umeå University

9 PUBLICATIONS 75 CITATIONS

[SEE PROFILE](#)



[Xu Shen](#)

Shanghai Institute of Materia Medica, Shang...

245 PUBLICATIONS 4,070 CITATIONS

[SEE PROFILE](#)



[Lihong Hu](#)

Chinese Academy of Sciences

213 PUBLICATIONS 2,690 CITATIONS

[SEE PROFILE](#)



[Y.T. Zheng](#)

Chinese Academy of Sciences

266 PUBLICATIONS 3,712 CITATIONS

[SEE PROFILE](#)

¹ Discovery of Inhibitors To Block Interactions of HIV-1 Integrase with ² Human LEDGF/p75 via Structure-Based Virtual Screening and ³ Bioassays

⁴ Guoping Hu,^{†,‡} Xi Li,^{†,‡} Xuan Zhang,^{‡,§} Yaozong Li,[†] Lei Ma,[†] Liu-Meng Yang,[‡] Guixia Liu,[†] Weihua Li,[†] Jin Huang,^{*,†} Xu Shen,[§] Lihong Hu,^{*,§} Yong-Tang Zheng,^{*,‡} and Yun Tang^{*,†}

⁶ [†]Shanghai Key Laboratory of New Drug Design, School of Pharmacy, East China University of Science and Technology, 130 Meilong Road, Shanghai 200237, China

⁸ [‡]Key Laboratory of Animal Models and Human Diseases Mechanisms of Chinese Academy of Sciences and Yunnan, Kunming Institute of Zoology, Chinese Academy of Sciences, Kunming 650223, China

¹⁰ [§]Shanghai Research Center for the Modernization of Traditional Chinese Medicine, Shanghai Institute of Materia Medica, Chinese Academy of Sciences, Shanghai 201203, China

¹² Supporting Information

ABSTRACT: This study aims to identify inhibitors that bind at the interface of HIV-1 integrase (IN) and human LEDGF/p75, which represents a novel target for anti-HIV therapy. To date, only a few such inhibitors have been reported. Here structure-based virtual screening was performed to search for the inhibitors from an *in-house* library of natural products and their derivatives. Among the 38 compounds selected by our strategy, 18 hits were discovered. The two most potent inhibitors showed IC₅₀ values at 0.32 and 0.26 μM, respectively. Three compounds were subsequently selected for anti-HIV assays, among which (*E*)-3-(2-chlorophenyl)-1-(2,4-dihydroxyphenyl)prop-2-en-1-one (NPD170) showed the highest antiviral activity (EC₅₀ = 1.81 μM). The antiviral mechanism of these compounds was further explored, and the results validated that the compounds interrupted the binding of transfected IN to endogenous LEDGF/p75. These findings could be helpful for anti-HIV drug discovery.

²² ■ INTRODUCTION

HIV-1 integrase (IN) is a vital enzyme that catalyzes the insertion of proviral DNA into the host cell genome, which has been validated as a potential target because of its essential role in viral replication.¹ The integration process of IN consists of two steps: 3'-processing and strand transfer. Raltegravir was the first FDA-approved drug that targeted HIV-1 IN in the strand transfer (ST) step. However, raltegravir-resistant HIV emerged soon afterward.² Ceccherini-Silberstein et al. confirmed that primary and secondary integrase inhibitor (INI)-associated mutations are absent or extremely rare in INI-naive patients. Conversely, a few specific IN polymorphisms found in INI-naive patients increased their frequency in antiretroviral-failing patients and/or are associated with RT resistance mutations.³ The emergence of viral strains resistant to clinically studied IN inhibitors demands the discovery of novel inhibitors that are structurally and mechanistically different.

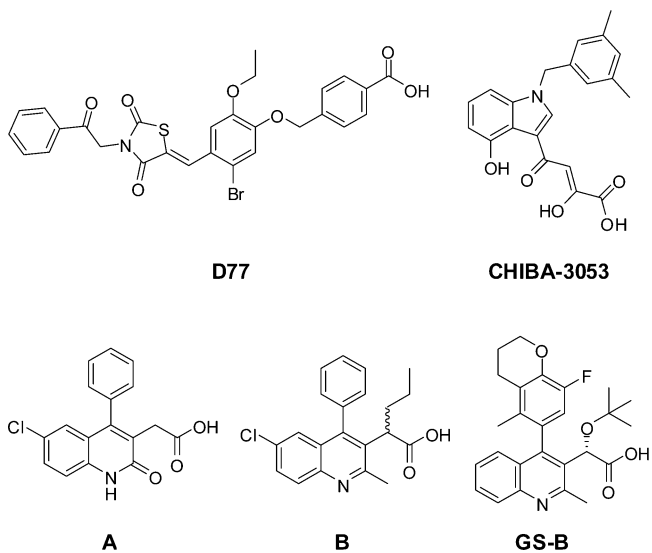
Protein–protein interaction inhibitors (PPIIs) could allow the discovery of drugs that can conquer the HIV-resistance.⁴ PPIIs are more resistant to spontaneous mutations at their binding sites. Several investigations have verified high conservation of amino acid residues within the contact interfaces compared with other regions of protein surfaces.^{5–7} Indeed, mutation at the interface of a single subunit within the protein–protein complex may affect proper functional protein assembly, which is especially important for antiviral drug design.⁸

Cellular cofactors are important for the integration function of IN.⁹ Among these cofactors, lens epithelial-cell-derived growth factor (LEDGF/p75) has been identified in complex with HIV-1 IN.^{10,11} LEDGF/p75 is essential in IN nuclear distribution, without which the HIV-1 virus cannot replicate.^{12,13} Therefore, disturbing or blocking IN–LEDGF/p75 interaction can prevent HIV-1 viral replication.^{14–17} LEDGF/p75-mediated chromatin tethering is critical for viral integration and dependent on specific interactions between the integrase-binding domain (IBD) of LEDGF/p75 and the IN core domain.¹⁴ Blocking IN–LEDGF/p75 interaction, a protein–protein interaction, provides a method of avoiding viral resistance and cross-resistance. Detailed interaction information between LEDGF/p75 IBD and the IN catalytic core domain (CCD) is provided by the complex crystal structure (PDB code: 2B4J), which allows rational design of inhibitors that block the binding of LEDGF/p75 to IN. The LEDGF/p75 IBD inserts into a relatively small and deep cleft at the IN dimer interface during IN–LEDGF/p75 interaction.¹⁵

In a previous report, we identified that compound D77 (see Chart 1), the first reported inhibitor to block IN–LEDGF/p75 interaction, can specially act on the IN dimer interface.¹⁸ A second inhibitor, C3003, was discovered by De Luca et al.¹⁹ with an IC₅₀ value of 35 μM, as tested by the AlphaScreen method. Subsequently, a series of compounds were developed

Received: August 23, 2012

Chart 1. Representative Structures of Inhibitors Targeting IN–LEDGF/p75 Interaction



74 based on compound C3003, among which compound CHIBA-
75 3053 showed an IC₅₀ value at 3.5 μM in the AlphaScreen assay
76 (see Chart 1).²⁰ Recently, 2-(6-chloro-2-oxo-4-phenyl-1,2-
77 dihydroquinolin-3-yl)acetic acid (compound A, see Chart 1)
78 and 2-(6-chloro-2-methyl-4-phenylquinolin-3-yl)pentanoic acid
79 (compound B, see Chart 1) were proven to bind to the
80 LEDGF/p75 binding pocket of IN through complex crystal
81 structures (PDB codes: 3LPT and 3LPU). These compounds
82 showed IC₅₀ values at 12 μM and 1 μM, respectively, through
83 the AlphaScreen assay.²¹ More recently, Tsiang et al.²² from
84 Gilead Sciences reported the most potent inhibitor GS-B
85 (Chart 1), which has an IC₅₀ value of 19 nM.

86 In the case of HIV-1 integrase, G140S/G148H and G148K
87 are common mutations arising during raltegravir therapy. Christ
88 et al.²³ demonstrated that inhibitors of IN–LEDGF/p75
89 interaction are not cross-resistant to INSTI-resistant mutants.
90 Inhibitors of IN–LEDGF/p75 interaction are potent inhibitors
91 of raltegravir-resistant virus strains. Compound B notably
92 retained its full activity against all five raltegravir-resistant
93 strains tested, underscoring its divergent mode of action.²¹

94 Natural products and their derivatives are always attractive
95 sources of lead discovery due to their diverse structural types
96 and thus may provide new perspectives for the design of IN–
97 LEDGF/p75 interaction inhibitors.²⁴ In the present study,
98 structure-based virtual screening (SBVS) was performed using
99 an induced-fit model to discover inhibitors that target IN–
100 LEDGF/p75 interaction from an *in-house* library of natural
101 products and their derivatives. Among the 38 compounds
102 selected by our strategy, 18 hits were identified as inhibitors
103 through AlphaScreen bioassays. Three compounds were further
104 tested *in vitro* for their anti-HIV-1 IN activity (EC₅₀) and
105 cytotoxicity (CC₅₀) in cell-based assays against HIV-1 IN
106 replication in acutely infected C8166 cells. In addition, the
107 effects of the inhibitors on IN intracellular distribution were
108 assayed on EGFP-fused IN-transfected 293T cells to identify
109 their anti-HIV mechanism. The results provide a solid
110 foundation for other investigations of inhibitors that target
111 IN–LEDGF/p75 interaction.

RESULTS

112

Structure-Based Virtual Screening. Figure 1 illustrates 113 the virtual screening process. The in-house library of natural 114

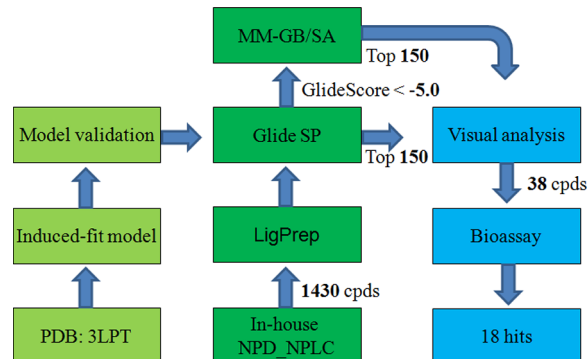


Figure 1. Schematic representation of hit discovery strategy.

products and derivatives in total contained 1430 compounds. 115 Figure 2 shows that the distribution of molecular weight, AlogP, 116 f2 and number of H-bond donors and acceptors are rather wide, 117 which indicate the diversity of the in-house natural products 118 and derivatives library. All the compounds were docked against 119 an induced-fit model of IN, named IFD_3LPT, which was 120 developed from a crystal structure (PDB code: 3LPT). 121 Although the resolution of 3LPT is fine (2.0 Å), it could not 122 yield a reasonable binding mode for most known active 123 compounds. Therefore, induced-fit docking was adopted to 124 adjust the binding pocket based on 3LPT. We found that an 125 induced-fit structure IFD_3LPT with a top IFD score could 126 yield a reasonable binding mode for most known active 127 compounds. Prior to database screening, it is crucial to test if a 128 model or scoring function can distinguish active compounds 129 from random compounds against a special target.²⁵ Model 130 validation indicated that IFD_3LPT could yield ROC enrich- 131 ment²⁶ higher than that of the two crystal structures, 3LPT and 132 3LPU, using both GlideScore and molecular mechanics- 133 generalized Born surface area (MM-GB/SA) score (Figure S1 134 in Supporting Information). Therefore, IFD_3LPT was 135 adopted as the virtual screening model in this study. The 136 difference between induced-fit mode and 3LPT was compared 137 and depicted in Figure S2 of Supporting Information. The main 138 chain in the binding pocket did not show obvious changes, 139 whereas the side chain of some key residues moved 140 significantly. The hydrophilic subpocket seems shortened with 141 the side-chain movement of residue Gln95 and Glu170. In 142 contrast, the hydrophobic subpocket seems enlarged with the 143 side-chain movement of residue Gln168 and Try132. After 144 docking, 150 compounds with top GlideScores and another 145 150 compounds with top MM-GB/SA scores were stored 146 separately for visual analysis after Glide standard precision (SP) 147 docking and MM-GB/SA calculation. Visual inspection was 148 adopted to check whether or not a compound created key 149 interactions with protein. This step makes sure that the selected 150 compounds have not only a higher score but also a reasonable 151 binding mode. Finally, 38 compounds were selected for 152 bioassays.

Bioassays at Molecular Level. The inhibitory activity of 154 selected compounds was determined using the AlphaScreen 155 assay to identify HIV-1 IN–LEDGF/p75 interaction inhibitors 156 with potential values as novel regulators of HIV-1 integration 157

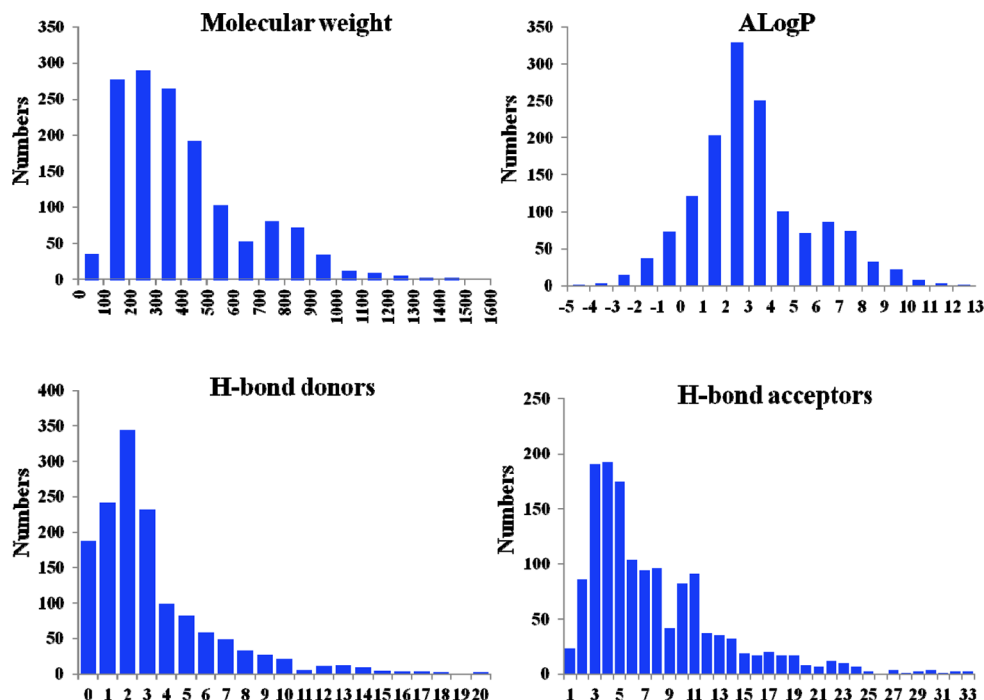


Figure 2. The distribution of molecular weight, AlogP, and number of H-bond donors and acceptors of the in-house natural products library.

158 (see the Experimental Section for details).²⁷ Results of the
159 bioassays are presented in Table 1. Among the 38 tested

interaction with an IC_{50} value at $12.2 \mu\text{M}$ by AlphaScreen assays,²¹ was purchased and used as a positive control.
160 Compound A showed an IC_{50} value at $11.65 \mu\text{M}$ in this study, approximating its previously reported value and thus confirming the accuracy and reliability of our bioassay. Five compounds even showed submicromolar inhibitory activity.
161 The chemical structures of the 18 active compounds are shown in Chart 2. All active compounds can be categorized into four types, namely chalcone, oleanolic acid, rosmarinic acid, and salicylamide. These inhibitors are structurally diverse, but most of them belong to chalcone derivatives and oleanolic acid derivatives; only one inhibitor was categorized as rosmarinic acid, and one was categorized as salicylamide.

The inhibition curves of the six representative compounds in AlphaScreen assays are shown in Figure 3, which demonstrated an unambiguous dose-dependent effect. Inhibition curves of the other active compounds are shown in Figure S3 of the Supporting Information. Among these inhibitors, two chalcone derivatives, namely compound 7 and (*E*)-3-(2,3-dihydroxyphenyl)-1-(2,4,6-trihydroxyphenyl)prop-2-en-1-one (NPD177), showed the most potent activities, with IC_{50} values at 0.32 and $0.26 \mu\text{M}$, respectively. Rosmarinic acid (NPLC0542) and two oleanolic acid derivatives, 3-(2-chlorophenyl)-2-((4*a*R,6*a*S,6*b*R,10*S*,12*a*R)-10-hydroxy-2,2,6*a*,6*b*,9,9,12*a*-heptamethyl-1,2,3,4,4*a*,5,6,6*a*,6*b*,7,8,8*a*,9-, 10,11,12,12*a*,12*b*,13,14*b*-icosahydron-4*a*-yl)pentanamido)-propanoic acid (NPD268) and (4*a*S,6*a*S,6*b*R,10*S*,12*a*R)-10-(benzyl oxy)-2,2,6*a*,6*b*,9,9,12*a*-heptamethyl-1,2,3,4,4*a*,5,6,6*a*,6*b*,7,8,8*a*,9,10,11,12,12*a*,12*b*,13,14*b*-icosahydron-4*a*-carboxylic acid (NPD297), showed relatively potent activities, with IC_{50} values at 0.55 , 0.65 , and $0.70 \mu\text{M}$, respectively. The salicylic-type compound, 4-(benzyloxy)-2-hydroxy-N-(3-nitrobenzyl)benzamide (NPD199), showed low micromolar activity. Some compounds did not display a normal sigmoidal curve which might due to the comparably narrow range of concentration. The different slopes might have relationships to the different characteristics of compounds.

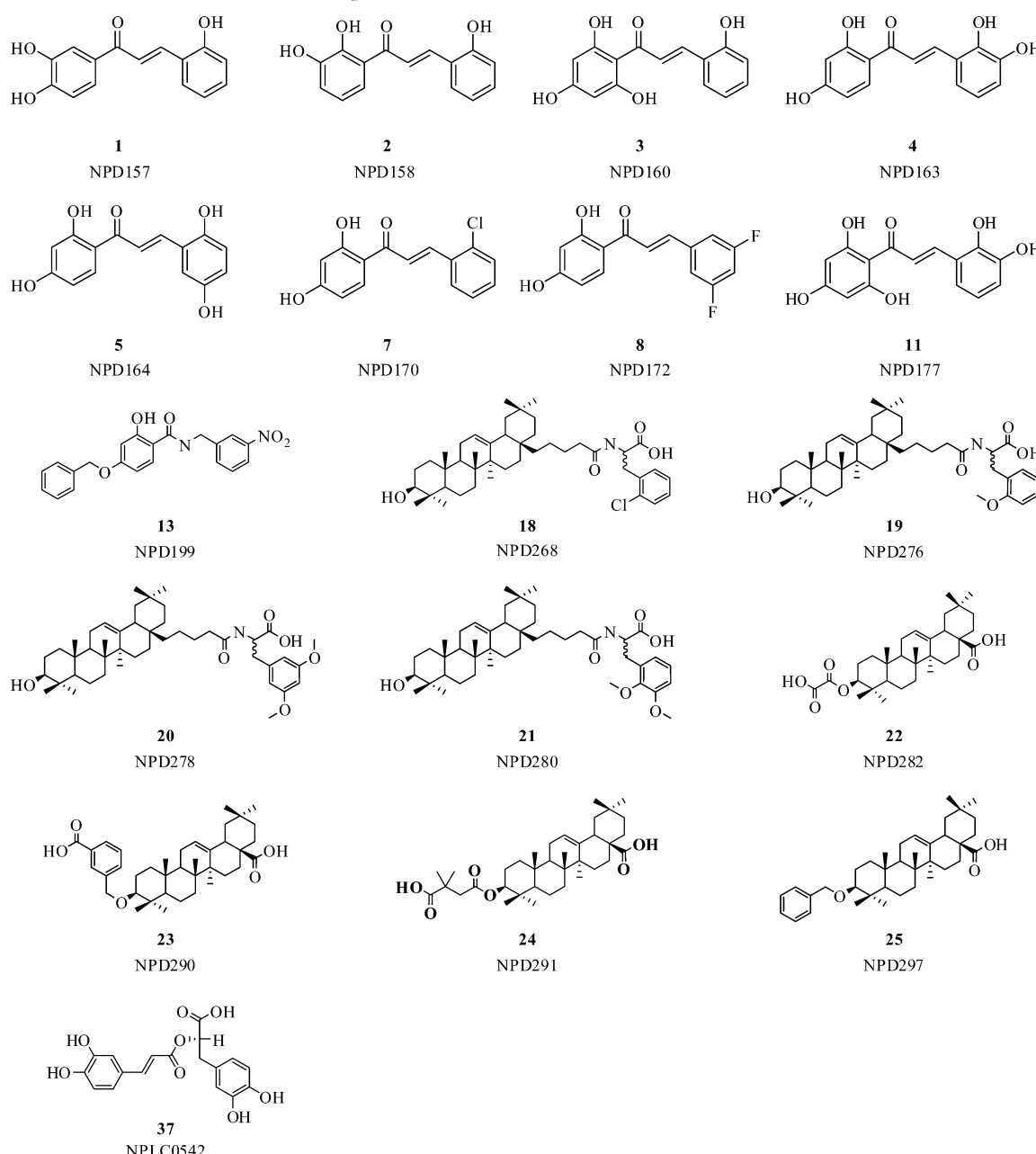
Table 1. Inhibitory Activities and cLogP and QPPCaco Values of 18 Active Compounds as well as Compound A

compound no.	$IC_{50}^a (\mu\text{M})$	cLogP ^b	QPPCaco ^c
1	3.67 ± 0.59	1.52	151.30
2	1.61 ± 0.22	2.18	216.74
3	6.21 ± 0.86	2.06	83.26
4	1.70 ± 0.26	1.42	64.83
5	3.78 ± 0.41	1.37	54.06
7	0.32 ± 0.06	3.27	470.68
8	1.75 ± 0.14	3.31	470.90
11	0.26 ± 0.05	1.36	29.93
13	3.84 ± 0.88	4.40	187.86
18	0.65 ± 0.05	9.39	86.69
19	4.56 ± 0.32	9.29	180.26
20	1.26 ± 0.11	9.29	108.43
21	3.22 ± 0.06	9.15	129.05
22	9.94 ± 3.08	6.12	10.63
23	1.14 ± 0.08	8.03	20.63
24	5.51 ± 0.97	7.57	20.45
25	0.70 ± 0.07	8.84	595.71
37	0.55 ± 0.14	1.15	1.65
compound A	11.65 ± 1.12	3.10	89.09

^aConcentration required inhibiting the HIV-1 IN-LEDGF/p75 interaction by 50%. ^bcLogP values of compounds were calculated with QikProp. ^cQPPCaco values of compounds were calculated with QikProp.

160 compounds, significant inhibitory activities were detected on 18
161 compounds, with IC_{50} values ranging from $0.26 \mu\text{M}$ to $9.94 \mu\text{M}$. In addition, original docking ranks prior to visual
162 inspection and candidate selection are provided in Table S2
163 of the Supporting Information. In the present study, compound
164 A, which was reported to block the IN-LEDGF/p75
165

Chart 2. Chemical Structures of Active Compounds



²⁰³ **Anti-HIV Activity and Cellular Toxicity.** Following the
²⁰⁴ remarkable activities of several inhibitors toward isolated HIV-
²⁰⁵ IN and LEDGF/p75, we further investigated the antiviral
²⁰⁶ activities of the three most promising inhibitors, compounds 7,
²⁰⁷ 11 (NPD177), and 18 (NPD268), on HIV-1_{IIIB}-infected C8166
²⁰⁸ cells. The cytopathic effect (CPE) was measured by counting
²⁰⁹ the number of syncytia under microscope, and the percentage
²¹⁰ inhibition of syncytia formation was calculated. 3'-Azido-3'-
²¹¹ deoxythymidine (AZT) was used as a positive control. Cellular
²¹² toxicity of compounds on C8166 cells was assessed by the 3-
²¹³ (4,5-dimethylthiazol-2-yl)-2,5-diphenyltetrazolium bromide
²¹⁴ (MTT) method (see Experimental Section). When these
²¹⁵ assays were utilized, the EC₅₀ and CC₅₀ values for compounds
²¹⁶ 7, 11, and 18 were determined from the dose-response curve
²¹⁷ (Figure 4A,B). Table 2 summarizes the antiviral testing results.
²¹⁸ All three compounds exhibited potent anti-HIV-1 activity, with
²¹⁹ EC₅₀ values at 1.81, 26.92, and 36.59 μM, respectively, and a

therapeutic index (TI) of 4.88, 3.76, and 2.12, respectively. ²²⁰
²²¹ Comparably narrow TIs indicate the necessity of further
²²² structural optimization to develop therapeutic drugs. ²²³

Effect of Inhibitors on EGFP-IN Intracellular Distribution. ²²³
²²⁴ EGFP-fused IN was transfected into 293T cells to
²²⁵ identify the effects of the compounds on IN intracellular
²²⁶ distribution. Transient expression of EGFP-IN resulted in a
²²⁷ significant nuclear localization (Figure 5A). Compound D77 ²²⁷ f5
²²⁸ was used as a positive control.¹⁸ Figure 5B-E shows that the
²²⁹ addition of D77 (83.83 μM), 7 (36.40 μM), 11 (86.73 μM),
²³⁰ and 18 (36.00 μM) affected the nuclear accumulation of
²³¹ EGFP-IN. Compared with EGFP-IN-transfected cells un-
²³² treated with D77, EGFP-IN appeared diffusely distributed in
²³³ the cytoplasm and almost no fluorescence could be observed in
²³⁴ the nucleus. Therefore, compounds 7, 11, and 18 may disrupt
²³⁵ IN nuclear distribution by interrupting the binding of
²³⁶ transfected IN to endogenous LEDGF/p75. ²³⁶

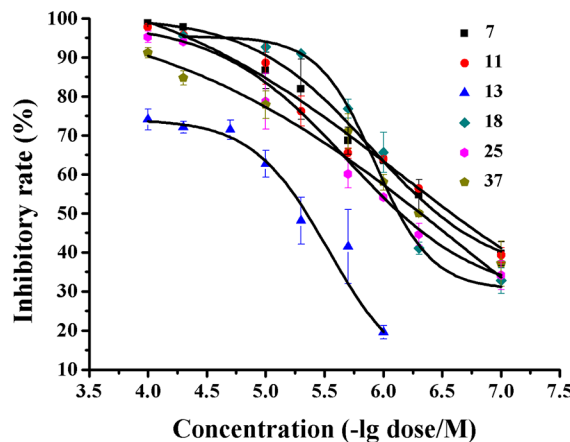


Figure 3. Dose–response curves of six representative IN–LEDGF/p75 interaction inhibitors in the AlphaScreen assay. Compound labels are listed on the right. The data of the AlphaScreen assay resulted from at least two independent experiments. Error bars represent the standard error of the mean (SEM).

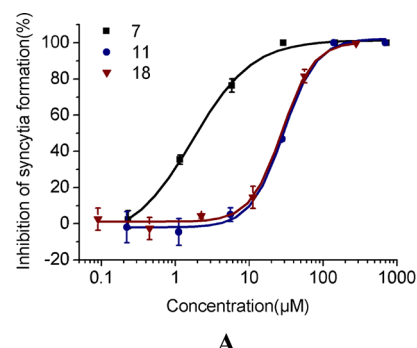
Table 2. Anti-HIV-1 Activity of Three Selected Compounds as well as AZT on C8166 Cells in Vitro

compound no.	EC_{50}^a (μM)	CC_{50}^b (μM)	TI^c
7	1.81 ± 0.14	8.83 ± 0.87	4.88
11	29.62 ± 0.56	111.33 ± 3.18	3.76
18	36.59 ± 8.85	77.51 ± 1.87	2.12
AZT ^{d)}	0.0087 ± 0.0004	4107.39 ± 616.18	473128.45

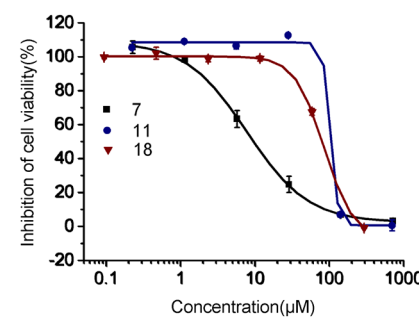
^a EC_{50} (50% effective concentration), concentration of test compound that reduces syncytia formation by 50%. ^b CC_{50} (50% cytotoxic concentration), concentration of test compound that causes 50% reduction in total C8166 cell number. ^c TI is a ratio of the CC_{50} value/ EC_{50} value. ^{d)}AZT was used as a positive control.

addition, Caco-2 cell permeability of these two compounds were predicted using QikProp.²⁸ Caco-2 cells are a model for the gut–blood barrier. QikProp predictions are for nonactive transport. The predicted Caco-2 cell permeability values for compounds 7 and 11 are 470.68 and 29.93, respectively, which indicated clearly that compound 7 has better cell permeability than compound 11.

Structure–Activity Analysis. A set of chalcone and oleanolic acid derivatives were selected and identified as inhibitors; therefore, the preliminary structure–activity relationship could be analyzed. For chalcone derivatives, the aromatic ring adjacent to the carbonyl group was named as A-ring and another aromatic ring was named as B-ring. Obviously, the inhibitory activities of chalcone derivatives are governed to a greater extent by the hydroxyl substituents on the A- and B-rings, and the most active compound is substituted with five hydroxyl groups (compound 11, $IC_{50} = 0.26 \mu M$). Comparing the active compound (*E*-3-(3,5-difluorophenyl)-1-(2,4-dihydroxyphenyl)prop-2-en-1-one (NPD172) with the inactive compound (*E*-1-(4-(benzyloxy)-2-hydroxyphenyl)-3-(3,5-difluorophenyl)prop-2-en-1-one (NPD182, Table S4), we found that the *p*-hydroxyl on ring A is needed for activity. Through the comparison among active compounds (*E*-3-(2,3-dihydroxyphenyl)-1-(2,4-dihydroxyphenyl)prop-2-en-1-one (NPD163), compound 11, and the inactive compound (*E*-1-(2,4-dihydroxyphenyl)-3-(2,6-dihydroxyphenyl)prop-2-en-1-one (NPD165, Table S4), we found that an additional *o*-hydroxyl group on the A-ring is favorable, whereas an additional *o*-hydroxyl group on the B-ring is unfavorable. With a chlorine group substituted on its B-ring, compound 7 shows the second highest inhibitory activity ($IC_{50} = 0.32 \mu M$), indicating that the hydroxyl substituents on the A-ring are more favorable and that



A



B

Figure 4. Dose–response curves of compounds 7, 11, and 18. (A) The EC_{50} of compounds were determined utilizing the C8166 cell line infected with HIV-1_{IIIB}. (B) The CC_{50} of compounds was determined utilizing the MTT-based cytotoxicity assay. The data of anti-HIV activities resulted from at least two independent experiments. Error bars represent the standard error of the mean (SEM).

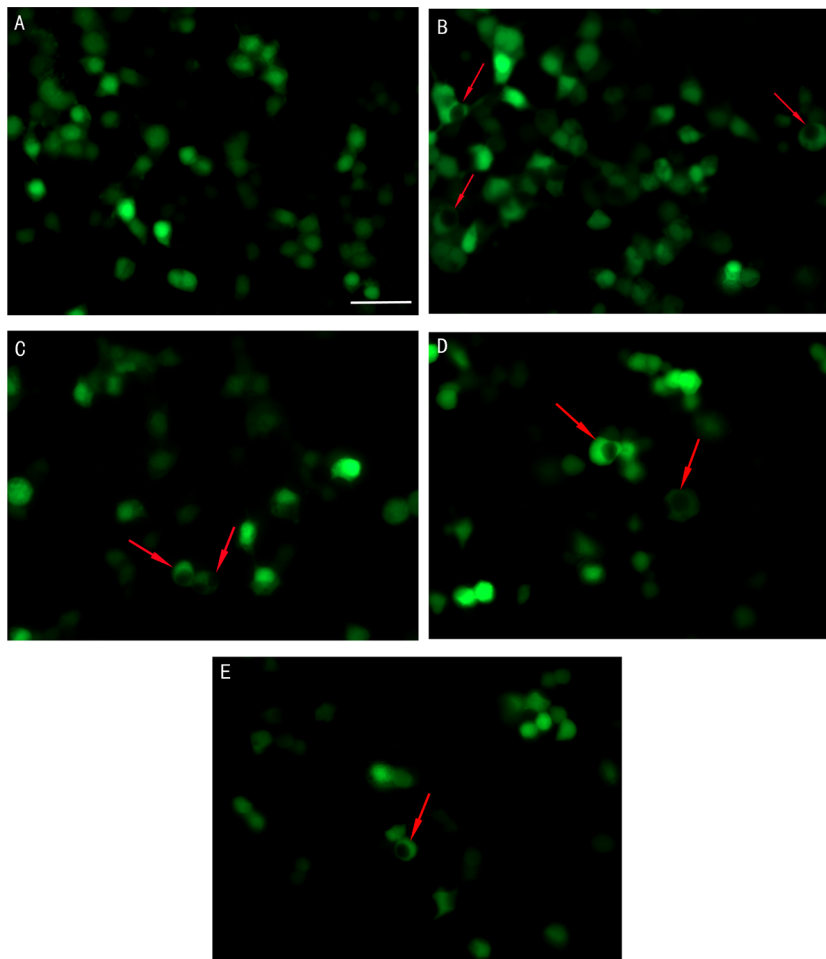


Figure 5. Effects of inhibitors on EGFP–IN nuclear distribution in 293T cells transformed with pEGFP–IN plasmid. (A) Without inhibitor, EGFP–IN was mainly distributed in the nucleus; (B) treated with 83.83 μM of D77, EGFP–IN was mainly distributed in the cytoplasm; (C) treated with 36.40 μM of compound 7; (D) treated with 86.73 μM of compound 11; (E) treated with 36.00 μM of compound 18. Red arrowheads show the EGFP–IN distribution. The scale bar is 50 μm .

the B-ring can be substituted by hydrophobic groups. As shown in Figure S1 of Supporting Information, model validation has been carried out using an external data set, which indicated that the induced-fit model could yield higher enrichment of active compounds under either GlideScore or MM-GBSA score. In this study, chalcone-type compounds were selected according to their higher GlideScore, because their polyhydroxyl ring can form hydrogen bonds with polar residues. Nevertheless, chalcone is a kind of α,β -unsaturated carbonyl compound and has the potential to act as a Michael acceptor. Therefore, chalcone should be carefully considered in the next study.

For oleanolic acid derivatives, the inhibitory activities are tolerant to both the inserted linker between the carboxyl group and ring and different substituents on the hydroxyl group. Four oleanolic acid derivatives including compound 18, 2-(5-((4aR,6aS,6bR,10S,12aR)-10-hydroxy-2,2,6a,6b,9,9,12a-heptamethyl-1,2,3,4,4a,5,6,6a,6b,7,8,8a,9,10,11,12,12a,12b,13,14b-icosahydropicene-4a-yl)pentanamido)-3-(2-methoxyphenyl)-propanoic acid (NPD276), 3-(3,5-dimethoxyphenyl)-2-(5-((4aR,6aS,6bR,10S,12aR)-10-hydroxy-2,2,6a,6b,9,9,12a-heptamethyl-1,2,3,4,4a,5,6,6a,6b,7,8,8a,9,10,11,12,12a,12b,13,14b-icosahydropicene-4a-yl)pentanamido)propanoic acid (NPD278), and 3-(2,3-dimethoxyphenyl)-2-(5-((4aR,6aS,6bR,10S,12aR)-10-hydroxy-2,2,6a,6b,9,9,12a-heptamethyl-1,2,3,4,4a,5,6,6a,6b,7,8,8a,9,10,11,12,12a,12b,13,14b-icosahydropicene-4a-yl)pentanamido)-3-(2-methoxyphenyl)-propanoic acid (NPD280) are structurally similar and differ only in terms of the substituted groups on their aromatic rings; all four oleanolic acid derivatives are racemic with respect to the α -carbon of the carboxylate group. Among the four derivatives, compound 18 yields the highest inhibitory activity, with chlorine substituted on the ortho-position. Substitution of a methoxyl group on the same position leads to a decrease in inhibitory activity. Docking results of the two chiral isomers of the four compounds indicated that the R-configuration might be favorable for their activity. Compared with the inactive R-configuration compound (R)-2-((4aS,6aS,6bR,8aS,10S,12aR,12bS,14bS)-10-hydroxy-2,2,6a,6b,9,9,12a-heptamethyl-1,2,3,4,4a,5,6,6a,6b,7,8,8a,9,-10,11,12,12a,12b,13,14b-icosahydropicene-4a-carboxamido)-3-phenylpropanoic acid (NPLC0783, Table S4), the linker between the pentacyclic system and amide seems necessary for activity.

Another four oleanolic acid derivatives including (4aS,6aS,6bR,10S,12aR)-10-(carboxycarbonyloxy)-2,2,6a,6b,9,9,12a-heptamethyl-1,2,3,4,4a,5,6,6a,6b,7,8,8a,9,-10,11,12,12a,12b,13,14b-icosahydropicene-4a-carboxylic acid (NPD282), (4aS,6aS,6bR,10S,12aR)-10-(3-carboxybenzyloxy)-2,2,6a,6b,9,9,12a-heptamethyl-1,2,3,4,4a,5,6,6a,6b,7,8,8a,9,-10,11,12,12a,12b,13,14b-icosahydropicene-4a-carboxylic acid (NPD290), (4aS,6aS,6bR,10-

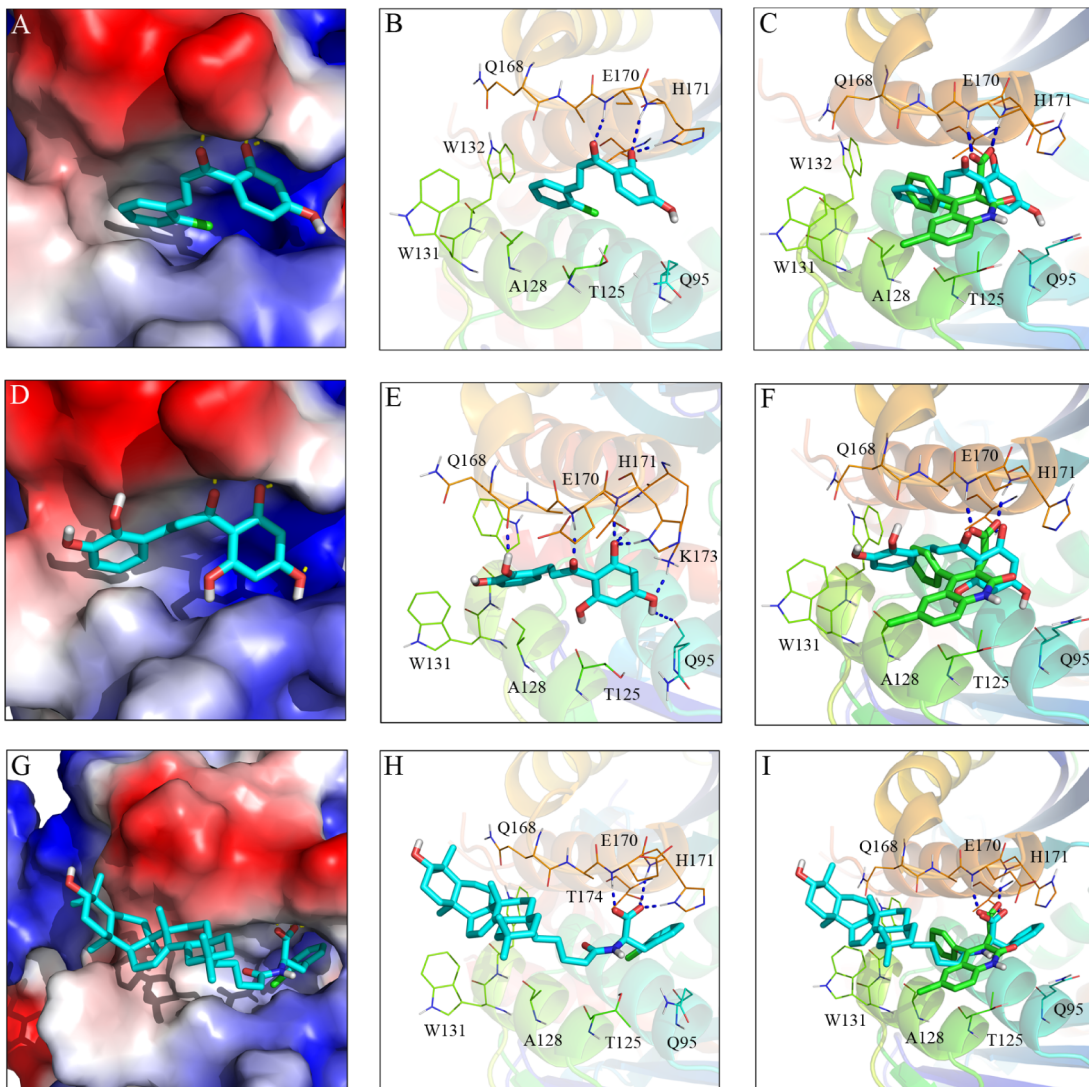


Figure 6. Putative binding modes of compounds **7** (A, B), **11** (D, E), and **18** (G, H) via IFD. The binding pocket of the enzyme was illustrated as (A, D, G) solvent-accessible surface colored by electrostatic potentials and (B, E, H) thin lines for key residues and light ribbon for others. Ligands are colored in cyan. Blue dashed lines represent H-bonding interactions between the ligand and receptor. The binding modes of the three inhibitors were superposed to compound A of crystal structure 3LPT (C, F, and I). These figures were prepared using PyMOL (<http://www.pymol.org/>).

343 *S*,12*aR*)-10-(3-carboxy-3-methylbutanoyloxy)-2,2,6*a*,6*b*,9,9,12*a*-
 344 heptamethyl-1,2,3,4,4*a*,5,6,6*a*,6*b*,7,8,8*a*,9,-
 345 10,11,12,12*a*,12*b*,13,14*b*-icosahydriopicene-4*a*-carboxylic acid
 346 (NPD291), and compound **25** (NPD297) have different
 347 substituted groups on the hydroxyl group. Among them,
 348 compound **25** has the highest inhibitory activity, indicating that
 349 hydrophobic groups are favorable at this position. Table 1
 350 shows that the calculated cLogP of all oleanolic acid derivatives
 351 range from 6.12 to 9.81, indicating that further optimization is
 352 necessary to develop druglike compounds.

353 With an extended structure, the oleanolic acid derivatives
 354 possess characteristics of PPIIs. Higher hydrophobic content
 355 and an extended interaction surface are favorable to disturb the
 356 protein–protein interaction. However, compared with oleanolic
 357 acid, chalcone has a very simple structure. The most potent
 358 chalcone derivative, compound **11**, can disturb protein–protein
 359 interaction at the submicromolar level. This result supports the
 360 idea that for some protein–protein interfaces, the affinity of the
 361 interaction is governed by a small, well-defined, compact
 362 subarea of a larger interface, namely the “hot spots”.⁸

Interestingly, while chalcone-type compounds have GlideScores 363 higher than those of oleanolic acid-type compounds, oleanolic 364 acid-type compounds have higher MM-GB/SA scores (Table 365 S2 of Supporting Information). All of the selected chalcone 366 derivatives contain at least one polyhydroxyl aromatic ring, 367 which may form more polar interactions with the appropriate 368 receptors and yield higher GlideScores. In contrast, the 369 oleanolic acid derivatives contain a pentacyclic triterpene core 370 structure that lacks polar interactions with receptors. However, 371 larger oleanolic acid derivatives can form more nonpolar 372 interactions and yield higher MM-GB/SA scores. This 373 observation provides new data and knowledge for future 374 screening and structural modification. 375

Binding Mode Analysis. IN is recognized by LEDGF/p75 376 through the following two key features: the specific backbone 377 conformation of residues 168–171, which can form a 378 hydrogen-bond network with IBD, and a hydrophobic patch 379 that accommodates the side-chain residues of LEDGF/p75, 380 namely Ile365, Phe406, and Val408.²⁹ The Asp366 of LEDGF/ 381 p75 forms a bidentate hydrogen bond with the main-chain 382

383 amides of the IN residues, Glu170 and His171, in chain A.
 384 Ile365 projects into a hydrophobic pocket formed by Thr174
 385 and Met178 in chain A as well as Leu102, Ala128, Ala129, and
 386 Trp132 in chain B. Using GRID molecular interaction fields,
 387 De Luca et al.²⁰ explored a hydrophobic region for ligand
 388 binding located near Trp131 in the B chain. Site mutagenetic
 389 studies also highlighted the role of Trp131.^{18,30}

390 Plausible binding modes of three representative compounds
 391 via induced-fit docking (IFD) are shown in Figure 6. The
 392 docking poses of compounds 7 and 11 reveal that the carbonyl
 393 group and the *o*-hydroxyl group of the A-ring form a hydrogen
 394 bond network with the main-chain amides of Glu170 and
 395 His171 and the side chain of His171 and Thr174 in chain A.
 396 Compound 11 forms additional hydrogen bonds with the side
 397 chain of Lys173 in chain A and the main chain of Gln95 in
 398 chain B. In particular, the phenolic hydroxyl group of the B-ring
 399 of compound 11 forms a hydrogen bond with the backbone of
 400 Gln168. The B-ring of both compounds is located in the
 401 hydrophobic pocket. The docking pose of compound 18
 402 reveals that the carboxyl group forms hydrogen bonding
 403 interactions with the main-chain amide of Glu170 and His171
 404 and the side chain of His171 and Thr174 in chain A. The
 405 triterpenoid skeleton of compound 18 occupies the hydro-
 406 phobic pocket. The superposition results indicated that the
 407 binding modes of the three inhibitors are very similar to that of
 408 the known inhibitor in the crystal structure. Especially, they all
 409 formed the characteristic bidentate hydrogen bond with the
 410 main-chain amide of Glu170 and His171.

411 ■ CONCLUSION

412 In the study, an in-house library containing natural products
 413 and their derivatives was virtually screened against an induced-
 414 fit model of HIV-1 integrase for new inhibitors to block IN–
 415 LEDGF/p75 interaction. Eighteen of the thirty-eight tested
 416 compounds were discovered as potent inhibitors via
 417 AlphaScreen assays, indicating the high success rate of this
 418 approach. The most potent compound 11 showed an IC₅₀
 419 value of 0.26 μM. Three compounds demonstrated significant
 420 anti-HIV activities. In particular, compound 7, which showed
 421 the highest anti-HIV activity, had an EC₅₀ value of 1.81 μM and
 422 a TI of 4.88. The three compounds also blocked IN nuclear
 423 distribution by interrupting the binding of transfected IN to
 424 endogenous LEDGF/p75. Compared with currently known
 425 active compounds, these newly identified inhibitors have
 426 significant potential for further development.

427 ■ EXPERIMENTAL SECTION

428 **Protein Preparation.** The crystal structure of HIV-1 IN CCD
 429 dimer complexed with compound A (PDB code: 3LPT) was used as a
 430 starting point to generate an induced-fit model of the enzyme.
 431 Compounds A, B, CX05045,²³ and CHIBA-3053 were employed in
 432 this process. IFD workflow of Maestro 9.0 was utilized with Prime
 433 2.1³¹ and Glide 5.5³² to adjust the receptor structure, especially in the
 434 binding pocket. All docking calculations were run in the “Standard
 435 Precision” (SP) mode of Glide, the center of the grid box was set to
 436 that of the ligand, and the box size was set to auto. All other
 437 parameters were left at default settings. All docked structures were
 438 automatically ranked according to their IFD score. The induced-fit
 439 structure with top IFD score was adopted in following virtual
 440 screening (named as IFD_3LPT).

441 **Ligand Preparation.** All compounds in the in-house library were
 442 prepared with Ligprep 2.3.³³ During this process, the OPLS_2005
 443 force field was chosen and the possible ionization states of each

compound at the pH range of 5.0–9.0 were generated. The cLogP and
 444 QPPCaco values of compounds were calculated with QikProp.²⁸

445 **Glide Docking and MM-GB/SA Rescoring.** The prepared small
 446 molecules were docked against IFD_3LPT using Glide SP with default
 447 settings.³⁴ After docking, the ligand–receptor binding free energy for
 448 each ligand was calculated using MM-GB/SA provided by the “Prime
 449 MM-GBSA” module.³¹ Only the top ranked molecules (GlideScore <
 450 –5.0) were submitted for MM-GB/SA calculation. All protein atoms
 451 were frozen, and only ligand structures were relaxed during MM-GB/
 452 SA calculation. The ligand strain energies were also calculated.³⁵

453 **Chemistry.** All test compounds were selected from the in-house
 454 library containing natural products and their derivatives. The syntheses
 455 of these compounds have been reported previously.^{36,37} The structures
 456 and purities of the 18 inhibitors were determined by ¹H NMR, mass
 457 spectra, and HPLC analysis (Table S3 of Supporting Information). ¹H
 458 NMR spectra were measured on a Bruker AM-400 or a Varian
 459 Mercury-VX300 spectrometer. ESI-MS was run on a Bruker Esquire
 460 3000 plus spectrometer in MeOH, and HR-ESI-MS was run on a
 461 Bruker Atex III spectrometer in MeOH. HPLC analysis used a Waters
 462 2695 Alliance LC System with a KR100-C18 Kromasil column (150 ×
 463 4.6 mm, 5 μm particle size), flow rate 1.0 mL/min; UV wavelength,
 464 210 or 254 nm. All tested compounds have a purity ≥95%.

465 **AlphaScreen Assay.** The inhibitory activities against the IN–
 466 LEDGF/p75 interaction were tested using AlphaScreen assays as
 467 described by Hou et al.²⁷ The HIV-1 IN CCD was expressed and
 468 purified as described by Jenkins et al.³⁸ The IBD of LEDGF/p75
 469 (residues 347–442) containing a GST tag was prepared as previously
 470 reported.¹⁸ Reactions were performed in a 25 μL final volume in
 471 well ProxiPlates (PerkinElmer). The buffer was composed of 25 mM
 472 HEPES, pH 7.3, 150 mM NaCl, 2 mM MgCl₂, 1 mM DTT, and 0.1%
 473 BSA. The His₆-tagged HIV IN CCD was added to a final
 474 concentration of 40 nM and incubated with test compounds at
 475 varying concentrations (0.1–100 μM) and room temperature for 30
 476 min. Subsequently, the remaining components containing a GST-
 477 tagged LEDGF/p75 IBD (final concentration, 40 nM), nickel chelate
 478 acceptor beads (final concentration, 8 μg/mL), and glutathione donor
 479 beads (final concentration, 8 μg/mL) were added to the well. Proteins
 480 and beads were incubated at room temperature for 2 h. The incubation
 481 was performed in the dark to avoid direct light exposure. The plates
 482 were measured with an EnVision Multilabel Plate Reader (PekinElm-
 483 er), with the final emission ranging from 520 to 620 nm.

484 **MTT-Based Cytotoxicity Assay.** Cellular toxicity of compounds
 485 on C8166 cells was assessed by MTT method as described
 486 previously.³⁹ Briefly, cells were seeded on 96-well microtiter plate in
 487 the absence or presence of various concentrations of compounds in
 488 triplicate and incubated at 37 °C in a humid atmosphere of 5% CO₂
 489 for 3 d. The supernatants were discarded, MTT reagent (12.1 mM in
 490 PBS) was added to each well and then incubated for 4 h, and 100 μL
 491 of 50% N,N-dimethylformamide (DMF)–20% SDS was added. After
 492 the formazan was dissolved completely, the plates were read on a Bio-
 493 Tek Elx 800 ELISA reader at 595/630 nm. The cytotoxic
 494 concentration that caused the reduction of viable C8166 cells by
 495 50% (CC₅₀) was determined from the dose–response curve.

496 **Anti-HIV Activity Assay.** C8166 cells (4×10^4 cells per well),
 497 infected with HIV-1_{IIB} at a multiplicity of infection (M.O.I. 0.15),
 498 were seeded on a 96-well plate in the absence or presence of various
 499 gradient concentrations of compounds in triplicate. The final volume
 500 per well was 200 μL. After 3 d of culture, the CPE was measured by
 501 counting the number of syncytia under microscope. Percentage
 502 inhibition of syncytia formation was calculated, and 50% effective
 503 concentration (EC₅₀) was calculated from the dose–response curve.
 504 AZT (Sigma) was used as a positive control. Therapeutic index (TI) =
 505 CC₅₀/EC₅₀. The data of anti-HIV activities resulted from at least two
 506 independent experiments, and the compounds were completely
 507 dissolved at the concentrations used in the experiment.

508 **EGFP-IN Intracellular Distribution Assay.** 293T cells were
 509 cultured and maintained in Dulbecco's modified Eagle's medium
 510 (DMEM) supplemented with 10% fetal bovine serum (FBS), 144.36
 511 μM G418, and 100 U/mL streptomycin–penicillin (Invitrogen) at 37
 512 °C in a 5% CO₂ incubator. Twenty-four hours before transfection,
 513

293T cells ($1 \times 105/\text{well}$) were seeded onto a clear 96-well plate in
 514 DMEM containing 10% FBS. 293T cells were transfected by EGFP-
 515 C-IN expression plasmid (The Chinese University of Hong Kong)
 516 using Lipofectamine 2000 reagent (Invitrogen). The medium was
 517 removed 5 h after transfection. Fresh medium containing compounds
 518 was added at different concentrations. Twenty-four hours after
 519 transfection, cells were fixed with 4% paraformaldehyde in PBS at
 520 room temperature for 15 min. Cell imaging was performed with a
 521 Leica DMI4000 microscope. D77 was used as a positive control.

523 ■ ASSOCIATED CONTENT

524 ■ Supporting Information

525 Model validation and docking ranks of active compounds and
 526 concentration–inhibition curves; ^1H NMR, mass spectra, and
 527 HPLC data of active compounds. This material is available free
 528 of charge via the Internet at <http://pubs.acs.org>.

529 ■ Accession Codes

530 2B4J, 3LPT, 3LPU.

531 ■ AUTHOR INFORMATION

532 ■ Corresponding Author

533 *(For J.H. and Y.T.) Tel.: +86-21-6425-1052, fax: +86-21-
 534 6425-3651, e-mail: huangjin@ecust.edu.cn; ytang234@ecust.
 535 edu.cn. (For L.H.) Tel.: +86-21-2023-1965, e-mail: simmhulh@
 536 mail.shcnc.ac.cn. (For Y.-T.Z.) Tel.: +86-871-519-5684, fax:
 537 +86-871-519-5684, e-mail: zhengyt@mail.kiz.ac.cn.

538 ■ Author Contributions

539 #These authors contributed equally to this work.

540 ■ Notes

541 The authors declare no competing financial interest.

542 ■ ACKNOWLEDGMENTS

543 This work was supported by the Program for New Century
 544 Excellent Talents in University (Grant NCET-08-0774), the
 545 Fundamental Research Funds for the Central Universities
 546 (Grant WY1113007), the Shanghai Committee of Science and
 547 Technology (Grant 11DZ2260600), the National Natural
 548 Science Foundation of China (grants 30925040 and
 549 81102483), and the Key Scientific and Technological Program
 550 of China (grants 2012ZX10001-006 and 2012ZX09103-101-
 551 022). The cDNA coding for HIV IN catalytic core domain
 552 (residues 50–212) including the F185K solubilizing-mutation
 553 was a gift from Prof. Robert Craigie (National Institutes of
 554 Health, Bethesda, MD). The full-length plasmid pCPNat p75
 555 was kindly provided by Prof. Zeger Debyser (Katholieke
 556 Universiteit Leuven, Belgium).

557 ■ ABBREVIATIONS USED

558 IN, integrase; CCD, catalytic core domain; IBD, integrase
 559 binding domain; VS, virtual screening; MM-GB/SA, molecular
 560 mechanics-generalized Born surface area; LEDGF, lens
 561 epithelial-cell-derived growth factor; MTT, 3-(4,5-dimethylth-
 562 iazol-2-yl)-2,5-diphenyltetrazolium bromide; PPIIs, protein–
 563 protein interaction inhibitors; ROC, receiver operating
 564 characteristics; IFD, induced-fit docking; CPE, cytopathic
 565 effect; AZT, 3'-azido-3'-deoxythymidine; TI, therapeutic
 566 index; cLogP, calculated log P ; EGFP, enhanced green protein;
 567 DTT, dithiothreitol; SDS, sodium dodecyl sulfate; BSA, bovine
 568 serum albumin; PBS, phosphate-buffered saline; MOI, multi-
 569 plicity of infection; CPE, cytopathic effect; PDB, Protein Data
 570 Bank

■ REFERENCES

- Anthony, N. J. HIV-1 integrase: A target for new AIDS chemotherapeutics. *Curr. Top. Med. Chem.* **2004**, *4*, 979–990.
- Malet, I.; Delelis, O.; Valantin, M. A.; Montes, B.; Soulie, C.; Wirden, M.; Tchertanov, L.; Peytavin, G.; Reynes, J.; Mouscadet, J. F.; Katlama, C.; Calvez, V.; Marcellin, A. G. Mutations associated with failure of raltegravir treatment affect integrase sensitivity to the inhibitor in vitro. *Antimicrob. Agents Chemother.* **2008**, *52*, 1351–1358.
- Ceccherini-Silberstein, F.; Malet, I.; Fabeni, L.; Dimonte, S.; Svicher, V.; D'Arrigo, R.; Artese, A.; Costa, G.; Bono, S.; Alcaro, S.; Monforte, A.; Katlama, C.; Calvez, V.; Antinori, A.; Marcellin, A. G.; Perno, C. F. Specific HIV-1 integrase polymorphisms change their prevalence in untreated versus antiretroviral-treated HIV-1-infected patients, all naive to integrase inhibitors. *J. Antimicrob. Chemother.* **2010**, *65*, 2305–2318.
- Al-Mawsawi, L. Q.; Neamati, N. Allosteric inhibitor development targeting HIV-1 integrase. *ChemMedChem* **2011**, *6*, 228–241.
- Arkin, M. R.; Wells, J. A. Small-molecule inhibitors of protein–protein interactions: Progressing towards the dream. *Nat. Rev. Drug Discovery* **2004**, *3*, 301–317.
- Caffrey, D. R.; Somaroo, S.; Hughes, J. D.; Mintseris, J.; Huang, E. S. Are protein–protein interfaces more conserved in sequence than the rest of the protein surface? *Protein Sci.* **2004**, *13*, 190–202.
- Veselovsky, A. V.; Archakov, A. I. Inhibitors of Protein-Protein Interactions as Potential Drugs. *Curr. Comput.-Aided Drug Des.* **2007**, *3*, 51–58.
- Wells, J. A.; McClendon, C. L. Reaching for high-hanging fruit in drug discovery at protein–protein interfaces. *Nature* **2007**, *450*, 1001–1009.
- Van Maele, B.; Busschots, K.; Vandekerckhove, L.; Christ, F.; Debys, Z. Cellular co-factors of HIV-1 integration. *Trends Biochem. Sci.* **2006**, *31*, 98–105.
- Cherepanov, P.; Maertens, G.; Proost, P.; Devreese, B.; Van Beeumen, J.; Engelborghs, Y.; De Clercq, E.; Debys, Z. HIV-1 integrase forms stable tetramers and associates with LEDGF/p75 protein in human cells. *J. Biol. Chem.* **2003**, *278*, 372–381.
- Ciuffi, A.; Llano, M.; Poeschl, E.; Hoffmann, C.; Leipzig, J.; Shinn, P.; Ecker, J. R.; Bushman, F. A role for LEDGF/p75 in targeting HIV DNA integration. *Nat. Med.* **2005**, *11*, 1287–1289.
- Llano, M.; Saenz, D. T.; Meehan, A.; Wongthida, P.; Peretz, M.; Walker, W. H.; Teo, W. L.; Poeschl, E. M. An essential role for LEDGF/p75 in HIV integration. *Science* **2006**, *314*, 461–464.
- Ciuffi, A.; Bushman, F. D. Retroviral DNA integration: HIV and the role of LEDGF/p75. *Trends Genet.* **2006**, *22*, 388–395.
- Al-Mawsawi, L. Q.; Neamati, N. Blocking interactions between HIV-1 integrase and cellular cofactors: an emerging anti-retroviral strategy. *Trends Pharmacol. Sci.* **2007**, *28*, 526–535.
- Poeschl, E. M. Integrase, LEDGF/p75 and HIV replication. *Cell. Mol. Life Sci.* **2008**, *65*, 1403–1424.
- De Rijck, J.; Vandekerckhove, L.; Gijsbers, R.; Hombrouck, A.; Hendrix, J.; Vercammen, J.; Engelborghs, Y.; Christ, F.; Debys, Z. Overexpression of the lens epithelium-derived growth factor/p75 integrase binding domain inhibits human immunodeficiency virus replication. *J. Virol.* **2006**, *80*, 11498–11509.
- Hombrouck, A.; De Rijck, J.; Hendrix, J.; Vandekerckhove, L.; Voet, A.; De Maeyer, M.; Witvrouw, M.; Engelborghs, Y.; Christ, F.; Gijsbers, R.; Debys, Z. Virus evolution reveals an exclusive role for LEDGF/p75 in chromosomal tethering of HIV. *PLoS Pathog.* **2007**, *3*, e47.
- Du, L.; Zhao, Y. X.; Chen, J.; Yang, L. M.; Zheng, Y. T.; Tang, Y.; Shen, X.; Jiang, H. L. D77, one benzoic acid derivative, functions as a novel anti-HIV-1 inhibitor targeting the interaction between integrase and cellular LEDGF/p75. *Biochem. Biophys. Res. Commun.* **2008**, *375*, 139–144.
- De Luca, L.; Barreca, M. L.; Ferro, S.; Christ, F.; Iraci, N.; Gitto, R.; Monforte, A. M.; Debys, Z.; Chimirri, A. Pharmacophore-Based Discovery of Small-Molecule Inhibitors of Protein-Protein Interactions between HIV-1 Integrase and Cellular Cofactor LEDGF/p75. *ChemMedChem* **2009**, *4*, 1311–1316.

- 640 (20) De Luca, L.; Ferro, S.; Gitto, R.; Barreca, M. L.; Agnello, S.;
641 Christ, F.; Debysyer, Z.; Chimirri, A. Small molecules targeting the
642 interaction between HIV-1 integrase and LEDGF/p75 cofactor. *Bioorg.*
643 *Med. Chem.* **2010**, *18*, 7515–7521.
- 644 (21) Christ, F.; Voet, A.; Marchand, A.; Nicolet, S.; Desimme, B. A.;
645 Marchand, D.; Bardiot, D.; Van der Veken, N. J.; Van Remoortel, B.;
646 Strelkov, S. V.; De Maeyer, M.; Chalatin, P.; Debysyer, Z. Rational
647 design of small-molecule inhibitors of the LEDGF/p75-integrase
648 interaction and HIV replication. *Nat. Chem. Biol.* **2010**, *6*, 442–448.
- 649 (22) Tsiang, M.; Jones, G. S.; Niedziela-Majka, A.; Kan, E.; Lansdon,
650 E. B.; Huang, W.; Hung, M.; Samuel, D.; Novikov, N.; Xu, Y.;
651 Mitchell, M.; Guo, H.; Babaoglu, K.; Liu, X.; Geleziunas, R.; Sakowicz,
652 R. New class of HIV-1 integrase (IN) inhibitors with a dual mode of
653 action. *J. Biol. Chem.* **2012**, *287*, 21189–21203.
- 654 (23) Christ, F.; Shaw, S.; Demeulementeester, J.; Desimme, B. A.;
655 Marchand, A.; Butler, S.; Smets, W.; Chalatin, P.; Westby, M.; Debysyer,
656 Z.; Pickford, C. Small-molecule inhibitors of the LEDGF/p75 binding
657 site of integrase block HIV replication and modulate integrase
658 multimerization. *Antimicrob. Agents Chemother.* **2012**, *56*, 4365–4374.
- 658 (24) Harvey, A. L. Natural products in drug discovery. *Drug Discovery*
659 *Today* **2008**, *13*, 894–901.
- 660 (25) Bissantz, C.; Folkers, G.; Rognan, D. Protein-based virtual
661 screening of chemical databases. 1. Evaluation of different docking/
662 scoring combinations. *J. Med. Chem.* **2000**, *43*, 4759–4767.
- 663 (26) Jahn, A.; Hinselmann, G.; Fechner, N.; Zell, A. Optimal
664 assignment methods for ligand-based virtual screening. *J. Cheminform.*
665 **2009**, *1*, 14.
- 666 (27) Hou, Y.; McGuinness, D. E.; Prongay, A. J.; Feld, B.; Ingravallo,
667 P.; Ogert, R. A.; Lunn, C. A.; Howe, J. A. Screening for antiviral
668 inhibitors of the HIV integrase - LEDGF/p75 interaction using the
669 AlphaScreen (TM) luminescent proximity assay. *J. Biomol. Screening*
670 **2008**, *13*, 406–414.
- 671 (28) QikProp, version 3.4, Schrödinger, LLC, New York, NY, 2011.
- 672 (29) Cherepanov, P.; Ambrosio, A. L. B.; Rahman, S.; Ellenberger,
673 T.; Engelman, A. Structural basis for the recognition between HIV-1
674 integrase and transcriptional coactivator p75. *Proc. Natl. Acad. Sci.*
675 U.S.A.
- 676 **2005**, *102*, 17308–17313.
- 677 (30) Busschots, K.; Voet, A.; De Maeyer, M.; Rain, J. C.; Emiliani, S.;
678 Benarous, R.; Desender, L.; Debysyer, Z.; Christ, F. Identification of the
679 LEDGF/p75 binding site in HIV-1 integrase. *J. Mol. Biol.* **2007**, *365*,
680 1480–1492.
- 681 (31) Prime, version 2.1, Schrödinger, LLC, New York, NY, 2009.
- 682 (32) Glide, version 5.5, Schrödinger, LLC, New York, NY, 2009.
- 683 (33) LigPrep, version 2.3, Schrödinger, LLC, New York, NY, 2009.
- 684 (34) Friesner, R. A.; Banks, J. L.; Murphy, R. B.; Halgren, T. A.;
685 Klicic, J. J.; Mainz, D. T.; Repasky, M. P.; Knoll, E. H.; Shelley, M.;
686 Perry, J. K.; Shaw, D. E.; Francis, P.; Shenkin, P. S. Glide: a new
687 approach for rapid, accurate docking and scoring. 1. Method and
688 assessment of docking accuracy. *J. Med. Chem.* **2004**, *47*, 1739–1749.
- 689 (35) Brooijmans, N.; Humblet, C. Chemical space sampling by
690 different scoring functions and crystal structures. *J. Comput.-Aided Mol.*
691 *Des.* **2010**, *24*, 433–447.
- 692 (36) Zhang, Y. N.; Zhang, W.; Hong, D.; Shi, L.; Shen, Q.; Li, J. Y.;
693 Li, J.; Hu, L. H. Oleanolic acid and its derivatives: new inhibitor of
694 protein tyrosine phosphatase 1B with cellular activities. *Bioorg. Med.*
695 *Chem.* **2008**, *16*, 8697–8705.
- 696 (37) Ma, L.; Yang, Z.; Li, C.; Zhu, Z.; Shen, X.; Hu, L. Design,
697 synthesis and SAR study of hydroxychalcone inhibitors of human beta-
698 secretase (BACE1). *J. Enzyme Inhib. Med. Chem.* **2011**, *26*, 643–648.
- 699 (38) Jenkins, T. M.; Engelman, A.; Ghirlando, R.; Craigie, R. A
700 soluble active mutant of HIV-1 integrase: involvement of both the core
701 and carboxyl-terminal domains in multimerization. *J. Biol. Chem.* **1996**,
702 *271*, 7712–7718.
- 703 (39) Zheng, Y. T.; Zhang, W. F.; Ben, K. L.; Wang, J. H. In vitro
704 immunotoxicity and cytotoxicity of trichosanthin against human
705 normal immunocytes and leukemia-lymphoma cells. *Immunopharma-*
706 *col. Immunotoxicol.* **1995**, *17*, 69–79.